Poststress Motionlike Artifacts Caused by the Use of a Dual-Head Gamma Camera for ^{201}Tl Myocardial SPECT

Oleg Blagosklonov, MD; Ahmad Sabbah, MD; Josette Verdenet, PhD; Michel Baud, PhD; and Jean-Claude Cardot, MD, PhD

Department of Nuclear Cardiology, Jean Minjoz University Hospital, Besançon, France

When performing ^{201}Tl myocardial SPECT using a dual-head gamma camera on patients after exercise stress, we have observed in some a sudden increase in the counting rate between the 16th and 17th images. This increase provoked motionlike artifacts, which increased the number of false-positive findings. The aim of our study was to determine possible causes for this leap in activity. **Methods:** We performed myocardial SPECT using a dual-head gamma camera on 110 patients after exercise stress: in 38 patients approximately 5 min after injection (group 1), in 43 patients approximately 14 min after injection (group 2), and in 29 patients twice, at approximately 5 and 20 min after injection (group 3). We also performed dynamic data acquisition for 10 min on 18 patients after exercise stress. We compared activity in the heart region in image series obtained after exercise stress and at rest. **Results:** Daily quality control tests eliminated the possibility of any malfunctions of the gamma camera. Careful image analysis showed no visible patient motion. Our results showed that upward creep of the heart could not be a cause of the described phenomenon. After exercise stress, a $\geq$5% activity leap in the heart region on the 16th and 17th frames was more frequent in group 1 than in group 2. Two consecutive acquisitions after exercise stress showed that the leap was >5% in 24 patients (83%) and 12 patients (41%) at the first and second acquisitions, respectively (group 3). In all patients, the leap was <5% at rest. Dynamic studies showed that the activity in the heart region steadily decreased in all patients after exercise stress. We suggest that decreasing ^{201}Tl concentrations in myocardium or blood could be a major reason for the described artifacts. **Conclusion:** We proposed that the pharmacokinetics of ^{201}Tl-chloride be evaluated within a short time after injection in humans after exercise stress. Now, in our department, we have begun acquisition approximately 12 min after ^{201}Tl administration, and the above-mentioned phenomenon has not appeared. However, to avoid the artifacts caused by early redistribution of ^{201}Tl, acquisition must not begin too late.

The accuracy of ^{201}Tl SPECT for assessing regional myocardial perfusion, that is, coronary artery disease, is well known, and its diagnostic and prognostic values are well established (*1–3*). However, SPECT may be associated with significant artifacts, and its accuracy can be limited by errors in data acquisition or image processing (*4–7*). Thus, daily quality control of gamma cameras is required to detect and prevent at least some of the artifacts, such as those caused by nonuniformity of detectors, center rotation errors, and misaligned camera heads (*4–7*)

Other types of artifacts, such as those resulting from motion of the patient or heart during tomographic acquisition, are unpredictable. The most frequent cause of these artifacts is voluntary or involuntary patient movement, which must be differentiated from vertical continuous motion of the heart during poststress acquisition—the so-called upward creep of the heart. This phenomenon was first described by Friedman at al. (*8*). Heart motion can be detected by careful image inspection in cine mode; the movement of even 1 pixel can provoke reconstruction errors and create artifacts that resemble anterior and posterior perfusion defects (*4–6*).

Today, multidetector SPECT systems are used in most nuclear medicine departments. Although dual- or triple-head gamma cameras present more quality control problems, their use shortens the acquisition and, as a result, reduces the risk of patient movement and consequent artifacts.

For some time, we have been using a dual-head gamma camera for ^{201}Tl myocardial SPECT with a standard protocol for data acquisition (the same protocol was applied previously to single-head gamma cameras), and we have been surprised by the increased number of false-positive
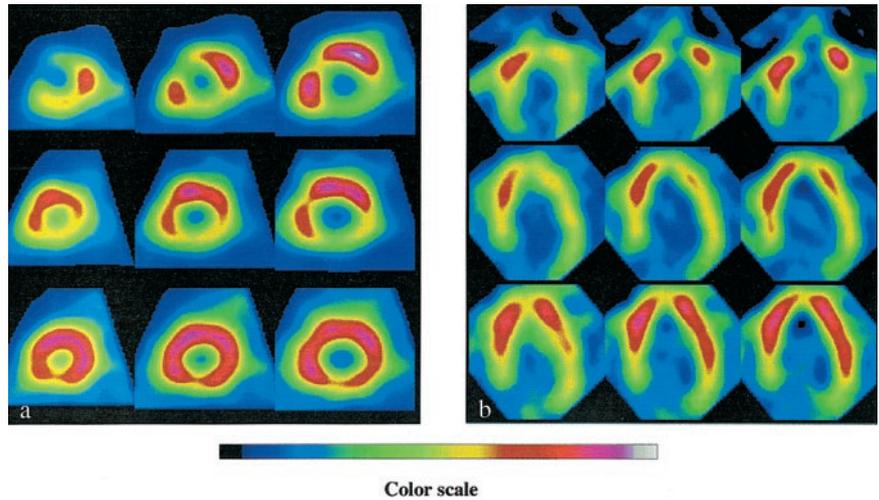
FIGURE 1. Short-axis (A) and vertical long-axis (B) images from same patient after exercise stress. Artificial perfusion defect was present on images obtained 5 min after ^{201}Tl injection (top) and disappeared on images obtained 13 min after injection (middle). This phenomenon never appeared at rest (bottom). Activity leap in heart region between 16th and 17th frames was 15%.

Color scale

findings. Although a previous study (9) reported that the incidence of false perfusion abnormalities was higher when dual-head gamma cameras were used, we wondered whether our gamma camera was malfunctioning or whether our acquisition protocol was inadequate.

Careful analysis of acquisition data showed, in some patients after exercise stress, a sudden increase in the counting rate between heart regions on the 16th and 17th frames (which correspond to passage from the first to the second detector). This phenomenon did not appear in these patients at rest (Fig. 1). The aim of our study was to determine whether this leap in activity was caused by patient movement, acquisition, or other errors.

MATERIALS AND METHODS

Data Acquisition

For the first phase of the investigation, 110 consecutive patients in whom no motion was detected during either poststress or rest imaging were studied. The clinical characteristics of the study population are presented in Table 1. For poststress imaging, the patients were divided into 3 groups. Data acquisition began approximately 5 min after injection in group 1 (38 patients) and approximately 14 min after injection in group 2 (43 patients). In group 3 (29 patients), imaging was performed twice—at approximately 5 and 20 min after injection. For rest imaging, data acquisition began approximately 18 min after injection in all patients.

Poststress and rest ^{201}Tl SPECT was performed with the patients supine. After exercise, a dose of 1.5 MBq/kg ^{201}Tl-chloride was administered intravenously; at rest, a dose of 0.9 MBq/kg was injected. The interval between poststress and rest imaging was at least 3 h. A rotating dual-head gamma camera (DST-XLi; SMV International, Buc, France) equipped with low-energy high-resolution collimators was used. The system detectors were set at 90°. The gamma camera was rotated in a contour orbit around the patient's chest through a 180° arc (32 projections, 40 s per projection) starting at 45° right anterior oblique. Data were stored in a 64 × 64 matrix, and 1.33 zoom was applied. The acquired raw scintigraphic data were preprocessed with a backprojection algorithm, and a Hann filter was applied.

For the second phase of the investigation, we performed a dynamic (sequential) data acquisition for 10 min (15 frames, 40 s per frame) on 18 patients after exercise stress. Imaging began at the 45° left anterior oblique position approximately 3 min after injection.

We also retrospectively selected 10 patients on whom poststress and rest ^{201}Tl SPECT was performed using a single-head gamma camera (DST-7; SMV International), applying the same acquisition protocol as was used in the dual-head studies. For these studies, the acquisition began 3–5 min after injection.

Data Analysis

For SPECT image sequences, we used a rectangular region of interest (ROI) (Fig. 2A) so that the heart was inside the ROI on each of the 32 frames. The ROIs corresponded to the matrix size (by X) and to the number of heart pixels (by Y). Activity curves
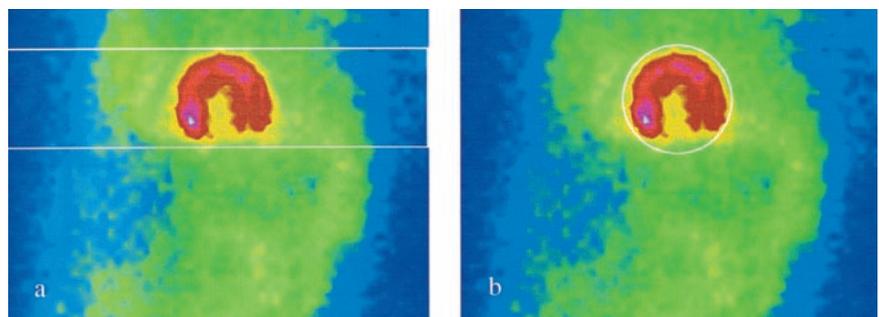

FIGURE 2. Rectangular (A) and circular (B) ROIs used for analysis in SPECT and dynamic studies.

were constructed for each ROI; we then compared activity in the ROIs on the 16th and 17th frames. The percentage of the leap was calculated according to:

$$P = \frac{A_{17} - A_{16}}{A_{16}} \times 100,$$

where P is the percentage of the leap, A_{16} is activity in the ROI on 16th frame, and A_{17} is activity in the ROI on 17th frame.

We also compared activity in the heart region on the 16th and 17th frames using a circular ROI (Fig. 2B) to eliminate the influence of upward creep. The ROI, manually adjusted, was centered on the heart on each image, but the size of the ROI was not changed. For image sequences obtained during dynamic studies, we constructed a time–activity curve for the heart region using a circular ROI (Fig. 2B).

For visual analysis, we normalized the curves by the activity value in the ROI on the first frame of the rest study (dual-head studies) and by the maximum activity value (single-head study).

Three independent observers visually interpreted the SPECT perfusion images from group 3 by dividing short-axis and vertical long-axis tomograms from each patient into 20 segments and scoring them with a 5-point system (0 = normal, 1 = equivocal, 2 = moderate, and 3 = severe reduction of radioisotope uptake and 4 = absence of detectable radiotracer in a segment) (10).

Data were expressed as mean $\pm$ SD. Patient data were compared using a 2-tailed t test for paired and unpaired data when appropriate.

Phantom Experiments

We used a phantom of the human chest and myocardium (Mayo Clinic, Rochester, MN). The phantom consisted of 3 chambers: 2 peripheral chambers simulating the lungs and a central chamber filled with a 18.5 MBq/L solution of ^{99m}Tc simulating the mediastinum with background noise. A myocardium chamber filled with a 148 MBq/L solution was fixed in the usual heart position in the central chamber. The scintigraphic data were acquired twice, using 25 s per frame and 120 s per frame. We used ^{99m}Tc because its half-life is shorter than that of ^{201}Tl, so that the radioactivity in the myocardial chamber could be decreased significantly in a relatively short time. The aim of these experiments was to prove that a decrease in activity in the heart region could provoke the leap in counts between the 16th and 17th frames.

TABLE 1
Clinical Characteristics of Patients

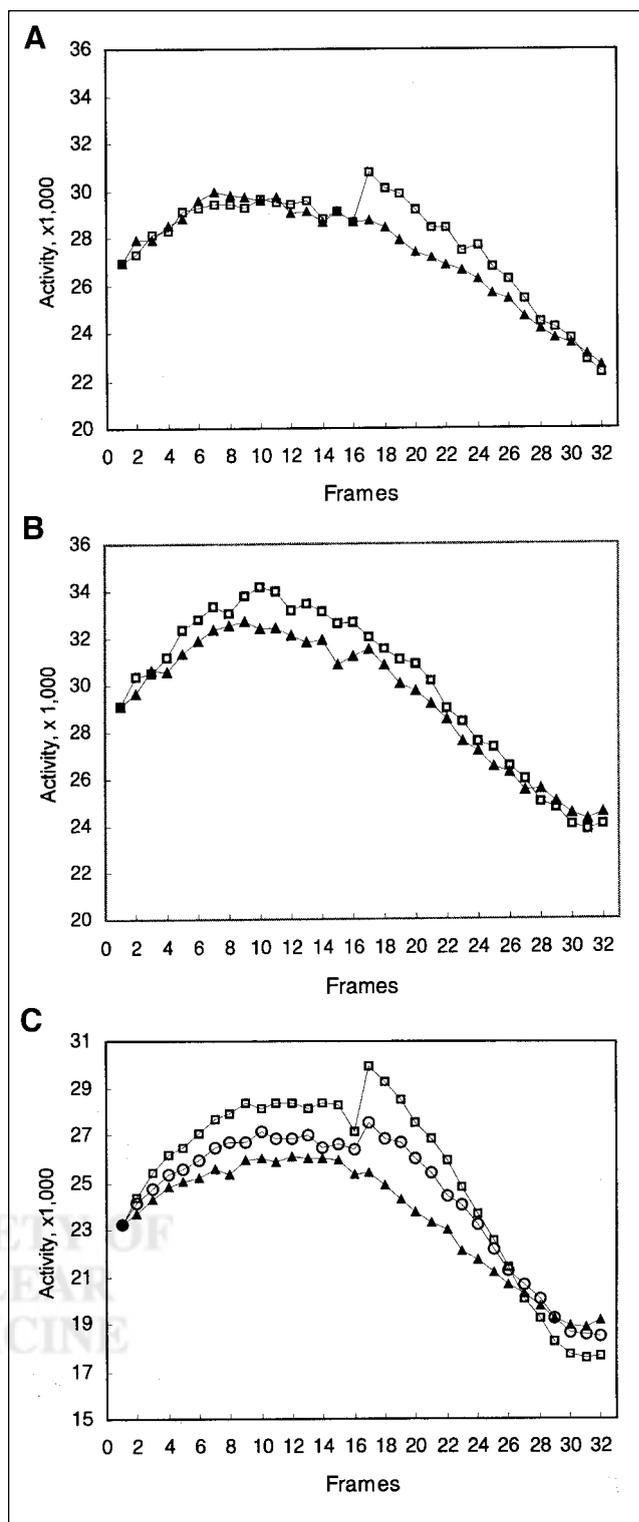| Characteristic	Group 1 ($n = 38$)	Group 2 ($n = 43$)	Group 3 ($n = 29$)
Age (y)	61 ± 8	60 ± 11	61 ± 9
Sex (M/F)	31/7	33/11	21/10
% of theoretic maximum heart rate	94 ± 8	98 ± 6	97 ± 7
Result of exercise stress test (positive/negative)	11/27	11/32	9/20
Perfusion abnormalities			
None	9	10	7
Reversible	15	19	12
Fixed	14	14	10

FIGURE 3. Representative activity curves for groups 1 (A), 2 (B), and 3 (C) approximately 5 min after exercise stress (□), approximately 20 min after exercise stress (○), and at rest (▲).

RESULTS

Daily quality control tests (center of rotation, uniformity, and interdetector alignment) and special tests (rotational uniformity, system sensitivity, and collimator hole align-

TABLE 2
Comparison of Leap in Different Groups of Patients

Time of imaging	Group 1 (n = 38)		Group 2 (n = 43)		Group 3 (n = 29)	
	>5%	>10%	>5%	>10%	>5%	>10%
After exercise*	26 (68%)	5 (13%)	19 (44%)	0	24 (83%) 12 (41%)	12 (41%) 0
At rest	0	0	0	0	0	0

*After exercise stress test, imaging was started approximately 5 min after injection in group 1 and approximately 14 min after injection in group 2, and myocardial SPECT was performed twice—at approximately 5 and 20 min after injection—in group 3.

ment) eliminated the possibility that the gamma camera had malfunctioned.

SPECT Studies

Figure 3 shows representative activity curves for each group of patients. In group 1, the leap in intensity between the 16th and 17th frames was 6.45% ± 3.31% and −1.17% ± 1.94% after exercise stress and at rest, respectively. In group 2, the leap was 4.38% ± 2.75 and 0.35% ± 2.90 after exercise stress and at rest, respectively. In group 3, the leap was 9.0% ± 3.70% at the first poststress acquisition, 4.53% ± 2.17% at the second poststress acquisition, and 0.11% ± 2.12% at rest; the mean difference between the leaps at the first and second poststress acquisitions was 4.51% ± 2.89%.

After exercise stress, the leap was >5% in 26 patients (68%) from group 1 and 19 patients (44%) from group 2, whereas at rest the leap was <5% in all patients from groups 1 and 2 (Table 2). Two consecutive acquisitions after exercise stress (group 3) showed that the leap was >5% in 24 patients (83%) and 12 patients (41%) at the first and second acquisitions, respectively; at rest, the leap was <5% in all patients (Table 2).

We found that the difference between the leaps after exercise stress and at rest was significant ($P < 0.001$) in all groups. In group 3, the difference between the values obtained at the first and second acquisitions after exercise stress was also significant ($P < 0.001$). The difference between the leaps after exercise stress in patients from group 1 and in patients from group 2 was not as great but was significant ($P = 0.004$).

The results obtained using a circular ROI confirmed those obtained using a rectangular ROI. The leap was often greater when a circular ROI was used.

The myocardial perfusion scores calculated by the 3 observers are summarized in Table 3. Differences between the scores at the first and second acquisitions were significant ($P < 0.01$) for all observers.

Dynamic Studies

Analysis of time–activity curves and tendency curves showed that activity in the heart region steadily decreased in all patients after exercise stress (Fig. 4). Activity in the heart region was significantly lower at the end of the acquisition (Fig. 5; $P < 0.001$). The mean slope was −21.65 ± 15.59.

Single-Head Studies

Visual analysis of the activity curves showed that, in all patients, activity in the heart ROI was greater after exercise stress than at rest in the first 15–20 frames but that afterward all curves matched perfectly (Fig. 6).

Phantom Experiments

Analysis of activity curves showed that the leap in counts between the 16th and 17th frames was 4% and 11% at the

TABLE 3
Perfusion Scores Obtained by 3 Observers in 2 Acquisitions

Patient no.	Observer 1		Observer 2		Observer 3	
	Acq 1	Acq 2	Acq 1	Acq 2	Acq 1	Acq 2
1	46	39	44	38	44	38
2	24	12	25	10	24	11
3	11	11	10	9	10	10
4	20	6	20	8	19	7
5	9	7	10	6	10	6
6	2	8	6	6	3	7
7	3	2	2	2	2	1
8	30	25	29	22	30	22
9	46	44	45	45	46	44
10	14	6	15	6	14	5
11	17	23	18	19	17	21
12	9	5	10	5	9	5
13	14	11	13	10	13	10
14	22	23	21	21	21	21
15	10	6	11	6	10	6
16	12	6	13	5	12	5
17	12	11	14	10	12	9
18	28	25	27	27	26	26
19	2	2	4	3	2	2
20	16	12	17	11	16	12
21	19	12	20	12	18	12
22	2	4	3	3	3	3
23	15	17	15	13	14	15
24	39	41	38	40	38	40
25	16	17	17	17	16	16
26	13	11	14	10	13	9
27	33	24	34	22	34	22
28	4	6	5	5	3	4
29	45	39	45	37	46	37

Myocardial SPECT was performed twice—at approximately 5 (Acq 1) and 20 min (Acq 2) after ^{201}Tl injection.
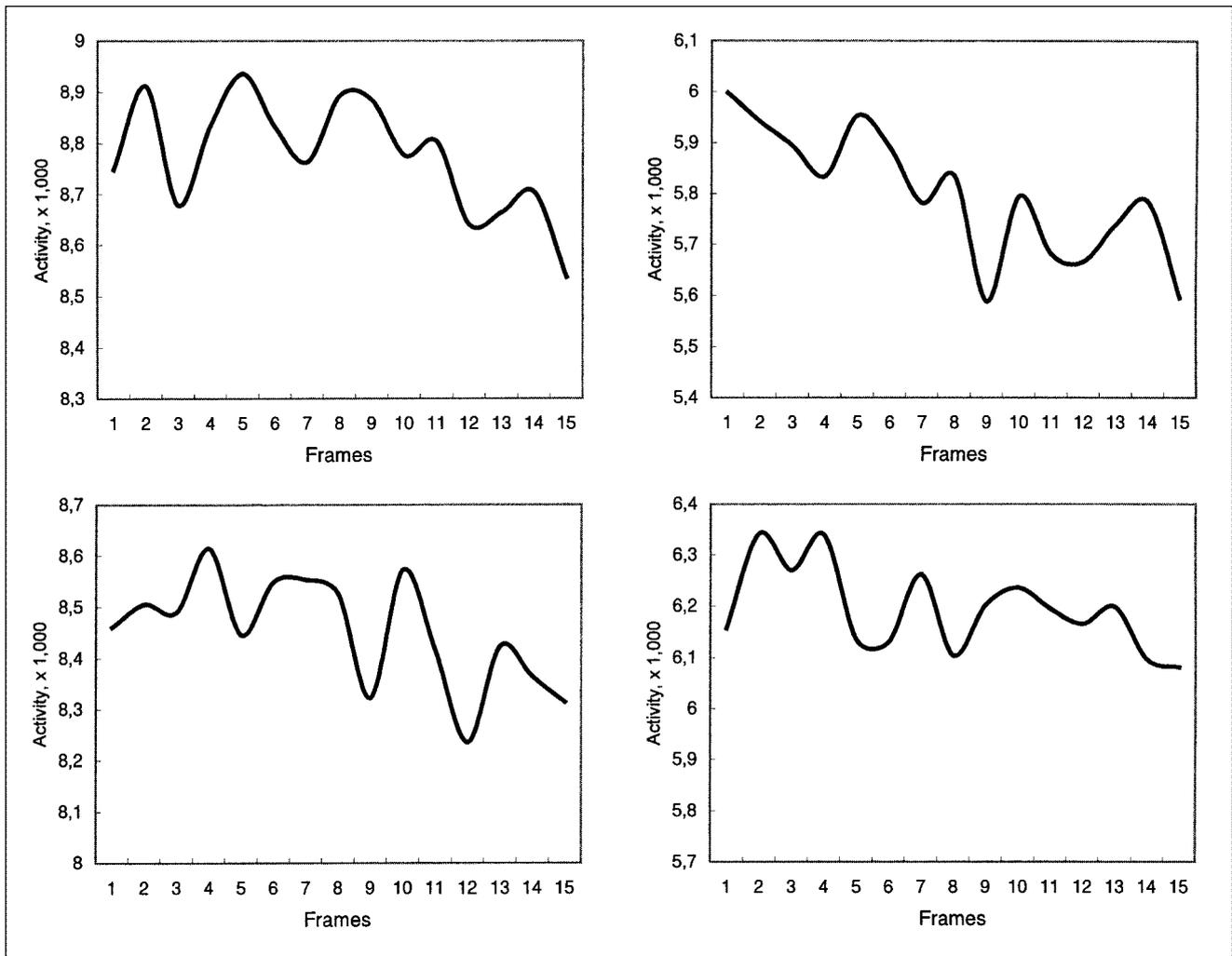
FIGURE 4. Examples of time–activity curves for heart ROI during 15 min after injection (4 patients).

first (25 s per frame) and second (120 s per frame) experiments, respectively.

DISCUSSION

We performed all recommended quality control tests (7) and some special tests (7), and no malfunctions of the gamma camera were detected. Furthermore, the leap in activity was present in a series acquired with a gamma camera from another manufacturer (data not shown), and our discussions with colleagues from other centers confirmed the existence and importance of the problem.

Patient motion is a frequent cause of artificial perfusion defects on myocardial SPECT scans (4–7). We evoked this hypothesis, but careful image inspection (visual analysis of projection views in a cine format and sinogram and linogram analysis) showed no visible patient motion.

Upward creep of the heart may be a cause of reconstruction artifacts (8,11,12). The frequency of this phenomenon has been estimated to be 16%–29% (8,11). In our study, a 5% leap in activity, which indicates a 1- or 2-pixel upward creep, was observed in 68%–83% of patients. Moreover,

the leap was detected in some patients >15 min after exercise stress; upward creep cannot last so long a time.

We applied a rectangular ROI because a rectangular ROI is generally used for backprojection. Of course, time–activity curves constructed using a rectangular ROI can be altered by a change in heart position or by background noise. However, the results obtained using a rectangular ROI strongly correlated with those obtained using a circular ROI, which could not have been affected by upward creep or background noise because the ROI was always centered on the heart.

Therefore, we hypothesized that the decrease in activity could be a major reason for the described phenomenon, because the 16th and 17th frames were acquired with an interval of approximately 10 min. The results of phantom experiments confirmed that decreasing activity caused by nuclear decay provokes the leap in counts.

The leap in activity was present only in poststress studies and was present then only if the acquisition was started relatively early after injection. This phenomenon never appeared in patients at rest; the acquisition began at least 15
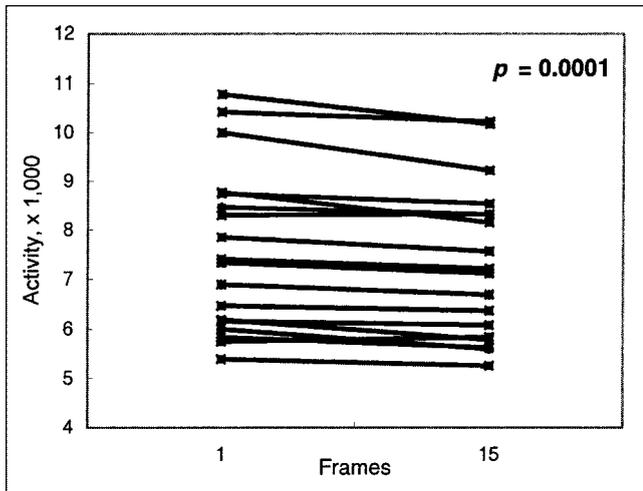
FIGURE 5. Difference in activity in heart region between first and 15th images in dynamic studies (18 patients).

min after injection. Therefore, we suggested that activity in the heart region becomes stable at approximately 15 min after injection.

Our dynamic studies showed that activity decreased for 10 min of the observation. However, we did not observe the plateau of activity. The results of single-head studies confirmed those of dynamic studies. Moreover, although the arc of the detector was the same in poststress and rest studies, there was an obvious difference between the shapes of the activity curves constructed for the heart region during the first 15–20 min. These findings support the hypothesis of an activity decrease.

Statistically significant differences between perfusion scores show that the described phenomenon affects clinical interpretation of images. This finding confirms the results of our visual analysis showing that the activity leap can provoke artificial perfusion defects.

The described leap in intensity could be a reason for the previously reported higher incidence of false-positive perfusion abnormalities detected by dual-head gamma cameras (*9*). We must also be vigilant about the presence of similar phenomena in gated SPECT studies.

Although ^{201}Tl is a radiotracer used in routine nuclear cardiology, there have been few studies on its pharmacokinetic distribution in humans (*13,14*). We suggest that more studies are necessary to measure ^{201}Tl distribution in humans after exercise stress, especially a short time after injection. These studies must answer the question of whether the decrease in activity in the heart region is caused by modifications of the ^{201}Tl blood concentration or by modifications of ^{201}Tl myocardial uptake and washout.

CONCLUSION

We cannot exclude the existence of poststress artifacts other than upward creep, and their influence on image reconstruction may be accentuated by the use of multi-

detector gamma cameras. The results of this study suggest that the decrease in activity in the heart region during the first 10 min after ^{201}Tl injection may induce artificial perfusion defects in some patients after exercise stress. Now, in our department, we have begun acquisition approximately
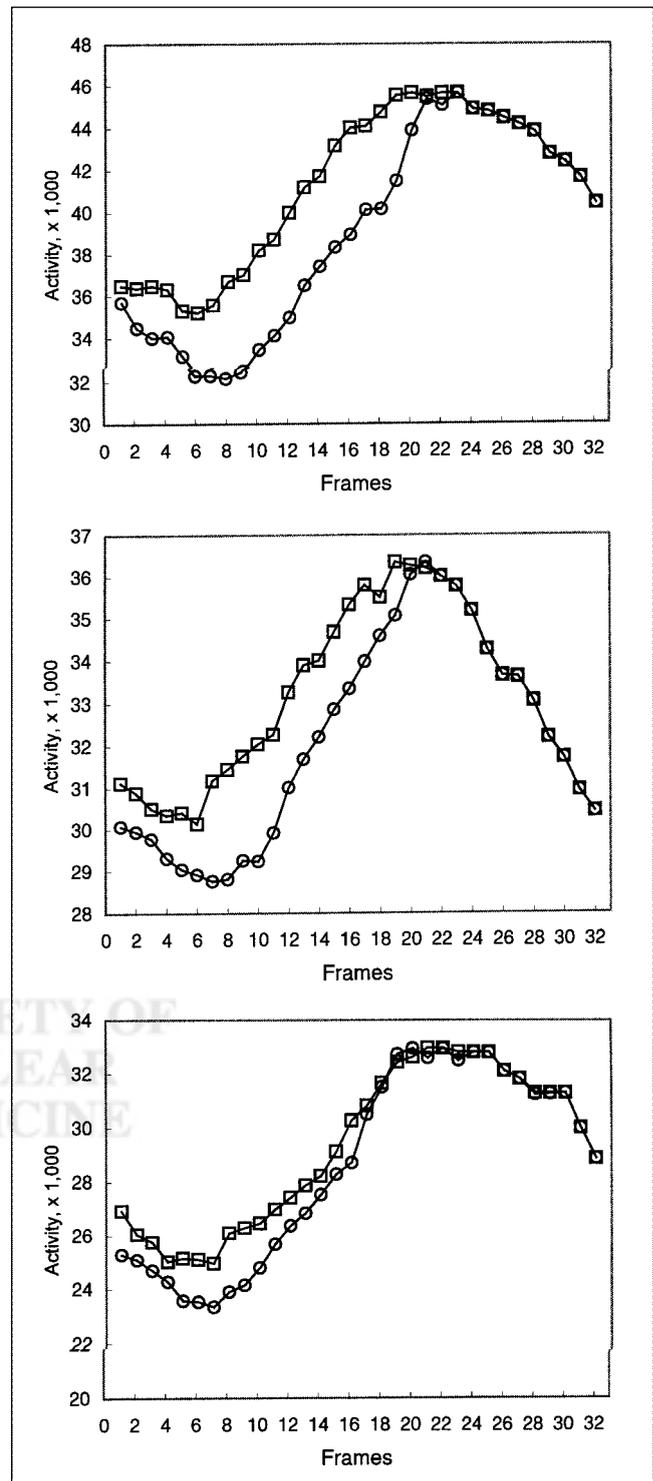

FIGURE 6. Examples of activity curves for heart ROI from image series obtained with single-head gamma camera (3 patients) after exercise stress (□) and at rest (○).

12 min after ^{201}Tl administration, and the above-mentioned phenomenon has not appeared. However, so that an inversion phenomenon (decrease in intensity between the 16th and 17th images) caused by early redistribution of ^{201}Tl can be avoided, acquisition must not begin too late.

ACKNOWLEDGMENTS

REFERENCES

1. Yao SS, Rozanski A. Principal uses of myocardial perfusion scintigraphy in the management of patients with known or suspected coronary artery disease. *Prog Cardiovasc Dis.* 2001;43:281–302.
2. Appelman YE, Piek JJ, van der Wall EE, et al. Evaluation of the long-term functional outcome assessed by myocardial perfusion scintigraphy following excimer laser angioplasty compared to balloon angioplasty in longer coronary lesions. *Int J Card Imaging.* 2000;16:267–277.
3. Shaw LJ, Hachamovitch R, Heller GV, et al., for the Economics of Noninvasive Diagnosis (END) Study Group. Noninvasive strategies for the estimation of cardiac risk in stable chest pain patients. *Am J Cardiol.* 2000;86:1–7.
4. DePuey EG. How to detect and avoid myocardial perfusion SPECT artifacts. *J Nucl Med.* 1994;35:699–702.
5. Geckle WJ, Frank TL, Links JM, Becker LC. Correction for patient and organ movement in SPECT: application to exercise thallium-201 cardiac imaging. *J Nucl Med.* 1988;29:441–450.
6. Wallis JW. Use of the selective linogram in cardiac tomography quality control. *J Nucl Cardiol.* 1995;2:303–308.
7. American Society of Nuclear Cardiology. Updated imaging guidelines for nuclear cardiology procedures: part 1. *J Nucl Cardiol.* 2001;8:G5–G58.
8. Friedman J, Van Train K, Maddahi J, et al. "Upward creep" of the heart: a frequent source of false-positive reversible defects during thallium-201 stress-redistribution SPECT. *J Nucl Med.* 1989;30:1718–1722.
9. Bax JJ, Visser FC, van Lingen A, Sloof GW, Cornel JH, Visser CA. Comparison between 360 degrees and 180 degrees data sampling in thallium-201 rest-redistribution single-photon emission tomography to predict functional recovery after revascularization. *Eur J Nucl Med.* 1997;24:516–522.
10. Hachamovitch R, Berman DS, Kiat H, et al. Exercise myocardial perfusion SPECT in patients without known coronary artery disease: incremental prognostic value and use in risk stratification. *Circulation.* 1996;93:905–914.
11. Mester J, Weller R, Clausen M, et al. Upward creep of the heart in exercise thallium 201 single photon emission tomography: clinical relevance and a simple correction method. *Eur J Nucl Med.* 1991;18:184–190.
12. He ZX, Darcourt J, Benoliel J, Migneco O, Magne J, Bussiere-Lapalus F. Major upward creep of the heart during exercise thallium-201 myocardial SPECT in a patient with chronic obstructive pulmonary disease. *J Nucl Med.* 1992;33:1846–1847.
13. Krahwinkel W, Herzog H, Feinendegen LE. Pharmacokinetics of thallium-201 in normal individuals after routine myocardial scintigraphy. *J Nucl Med.* 1988;29:1582–1586.
14. Takahashi N, Reinhardt CP, Marcel R, Leppo JA. Myocardial uptake of ^{99m}Tc-tetrofosmin, sestamibi, and ^{201}Tl in a model of acute coronary reperfusion. *Circulation.* 1996;94:2605–2613.